



## Application of Image Processing for Detection and Classification of Malignant and Benign Breast Cancer Tissues

Hala Moustafa<sup>1</sup>, Metwally Kotb<sup>2</sup>, Heba Ramadan<sup>2</sup>, Diana El-Sherif<sup>3</sup>

<sup>1</sup>Medical Biophysics and Biomedical Equipment's, Faculty of Applied Medical Sciences, October 6

University.<sup>2</sup>Medical Biophysics, Medical Research Institute, University of Alexandria.

<sup>3</sup>Radiology Department, Faculty of Applied Medical Sciences.

**Abstract: Objective:** To compare between images obtained by two modalities employing two software programs as a trial to obtain solid conclusion of using either of these modalities for the better differentiation between benign and malignant breast tumors. **Methods:** A total of 60 female breast patients were enrolled, in addition to 10 control female with no symptoms of breast disease. The patients were divided into two main groups; one group of benign and the other of malignant breast changes. All groups were submitted to mammography and ultrasound breast examination. In mammography, two routine views; a top-to-bottom CC view and an oblique side MLO view were recorded. Photo Shop 7.0 ME Software and MATLAB Software were employed, based on the gray-level histogram, to describe the obtained data. **Results:** Gray level histogram in benign breast tissue appears as a broad peak at the middle with sharp top and more area, in mammography, as a peak with broad base and sharp top, shifted and skewed (-) to left, in ultrasonography. Malignant tissue, appears as: a broad peak at the middle, with broad base and broad top, in mammography, as a peak with sharp top extends from the middle, shifted and skewed (-) to left, in ultrasonography, and as a peak of gradual increase in intensity forming sharp peak at the lower end of the histogram. The sensitivity increases on the expense of specificity, and vice versa.

[Hala Moustafa, Metwally Kotb, Heba Ramadan, Diana El-Sherif. **Application of Image Processing for Detection and Classification of Malignant and Benign Breast Cancer Tissues.** *Cancer Biology* 2020;10(2):18-28]. ISSN: 2150-1041 (print); ISSN: 2150-105X (online). <http://www.cancerbio.net>. 4. doi:[10.7537/marscbj100220.04](https://doi.org/10.7537/marscbj100220.04).

**Keywords:** Images Processing -Benign Breast Cancer -Malignant Breast Cancer - Photo Shop 7.0 ME Software - MATLAB Software – Mammography- Ultrasonography

### Introduction:

Breast cancer is the most common malignancy in women around the world. Information on the incidence and mortality of breast cancer is essential for planning health measures. <sup>(1)</sup>Detection and diagnoses of breast cancer early and getting state-of-the-art cancer treatment are the most important strategies to prevent deaths from breast cancer. Breast cancer that's found early, when it's small and has not spread, is easier to treat successfully. Getting regular screening tests is the most reliable way to find breast cancer early. The American Cancer Society has screening guidelines for women at average risk of breast cancer, and for those at high risk for breast cancer. <sup>(2,3)</sup>

Mammography is essentially the only widely used imaging modality for breast cancer screening. It is effective in reducing breast cancer mortality rates in numerous studies. Mammography exposes the breasts to small amounts of radiation. But the benefits of mammography outweigh any possible harm from the radiation exposure. Doctor reading the mammogram looking for different types of breast changes, such as small white spots called calcifications, either macro or

micro calcifications, lumps or tumors called masses, and other suspicious areas that could be signs of cancer. When possible, the doctor reading the mammogram will compare it to old mammograms of the patient. This can help show if any findings are new, or if they were already there on previous mammograms. Findings that haven't changed from older mammograms aren't likely to be cancer, which might mean that patient won't need further tests.

Ultrasonography is now a major mode of imaging for the clinical diagnosis of breast cancer. Breast ultrasonography have been the improved benign/malignant differentiation of solid breast lesions and the use of US to guide interventional procedures such as needle aspirations, core-needle biopsies, and pre-biopsy needle localizations of breast masses or calcifications. <sup>(4,5)</sup>

### Aim Of The Work:

The aim of the present work is the application of images processing and evaluation techniques for detection and classification of benign and malignant breast cancer tissues.

**Materials And Methods:****1-Patients:**

A total of 60 female breast patients were enrolled in this study, in addition to 10 control female (with no symptoms of breast disease). The breast patients were divided into two main groups. One group was of benign breast tumors (30) and the other group of malignant breast changes (20). All groups (including the control group) was submitted to mammographic, and ultrasound breast examination. Each group was submitted to digital Mammography (General Electric) and Ultrasound (Toshiba) devices. Patients were diagnosed at the Cairo Scan Women Imaging Units, El-Giza, Egypt. A written informed consent was obtained from each female's patient for performing either the digital mammography or ultrasound.

**2- Procedure of Digital Mammography:**

During Digital Mammography, the breast is compressed by a dedicated digital mammography machine to even out the tissue, to increase image quality, and to hold the breast still (preventing motion blur). Both front and side images of the breast are taken. Until some years ago, digital mammography was typically performed with screen-film cassettes. The breast is placed on a special plat form and compressed with a paddle (often made of clear Plexiglas or other plastic). The technologist gradually compresses the breast. The patient was asked to change positions between images. The routine views are a top-to-bottom view (CC view) and an oblique side view (MLO view).

**3- Procedure of Ultrasonography:**

Ultrasound examinations do not use ionizing radiation (as used in x-rays), thus there is no radiation exposure to the patient. Because ultrasound images are captured in real-time, they can show the structure and movement of the body's internal organs, as well as blood flowing through blood vessels. Ultrasound imaging can help to determine if an abnormality is solid (which may be a non-cancerous lump of tissue or a cancerous tumor) or fluid-filled (such as a benign cyst) or both cystic and solid. The patient lie on her

back on the examining table and may be asked to raise her arm above her head. After she is positioned on the examination table, the radiologist (a physician specifically trained to supervise and interpret radiology examinations) or sonographer applies a warm water-based gel to the area of the body being studied. The gel will help the transducer make secure contact with the body and eliminate air pockets between the transducer and the skin that can block the sound waves from passing into the body. The transducer is placed on the body and moved back and forth over the area of interest until the desired images are captured.

**4-Photo Shop 7.0 ME Software:**

Photo shop 7.0 software is a program that was used to describe the obtained data. The method for the analysis of breast composition was accomplished using transforms pixel values. Pixel uniformity is another important consideration that impacts the accuracy and integrity of the image, which can also influence the presence of noise. Each image was divided into 512 x 512 pixels.

**5-Validation Measures:**

Sensitivity and specificity are statistical measures of the performance of a binary classification test. Sensitivity (also called the true positive rate), measures the proportion of actual positives which are correctly identified as such (e.g. the percentage of sick people who are correctly identified as having the condition). The test results for each subject may or may not match the subject's actual status. In that setting: True positive (TP): Sick people correctly diagnosed as sick False positive (FP): Healthy people incorrectly identified as sick True negative (TN): Healthy people correctly identified as healthy False negative (FN): Sick people incorrectly identified as healthy. Sensitivity relates to the test's ability to identify positive results. The sensitivity of a test is the proportion of people that are known to have the disease who test positive for it. This can also be written as:

$$\text{sensitivity} = \frac{\text{number of true positives}}{\text{number of true positives} + \text{number of false negatives}}$$

$$= \text{probability of a positive test, given that the patient is ill}$$

**Specificity relæ**

s:

$$\text{specificity} = \frac{\text{number of true negatives}}{\text{number of true negatives} + \text{number of false positives}}$$

$$= \text{probability of a negative test given that the patient is well}$$

A sensitivity of 100% means that the test recognizes all actual positives – i.e. all sick people are recognized as being ill. Thus, in contrast to a high specificity test, negative results in a high sensitivity test are used to rule out the disease. <sup>(6)</sup>

### 6-Statistical Analysis:

Continuous variables were recorded as mean  $\pm$  SD; ANOVA-f test, followed by Tukey's test, was used to evaluate the significance of difference ( $P < 0.05$ ) among group. Data were expressed as mean  $\pm$  standard error (S.E). Data analysis was made by using statistical SPSS -12 programs for Widows (Chicago, IL, USA) when appropriate ( $P < 0.05$ ) was considered statistically significant. Histogram analysis combines techniques that compute statistics and measurements based on the gray-level intensities of the image pixel.

### 7-Matlab Software:

To calculate the gray-level co-occurrence matrix for a gray scale image, the MATLAB® gray Comtrex [90] package was used to evaluate the following values:

#### Mean

The mean,  $m$  of the pixel values in the defined window, estimates the value in the image in which central clustering occurs. The mean can be calculated using the formula:

$$\mu = \frac{1}{MN} \sum_{i=1}^M \sum_{j=1}^N p(i, j)$$

Where  $p(i, j)$  is the pixel value at point  $(i, j)$  of an image of size  $M \times N$ .

#### Standard Deviation

The Standard Deviation,  $\sigma$  is the estimate of the mean square deviation of grey pixel value  $p(i, j)$  from its mean value  $m$ . It is determined using the formula:

$$\sigma = \sqrt{\frac{1}{MN} \sum_{i=1}^M \sum_{j=1}^N (p(i, j) - \mu)^2}$$

#### Skewness

Skewness,  $S$  characterizes the degree of asymmetry of a pixel distribution in the specified window around its mean. The formula for finding Skewness is given in the below equation:

$$S = \frac{1}{MN} \sum_{i=1}^M \sum_{j=1}^N \left( \frac{p(i, j) - \mu}{\sigma} \right)^3$$

Where,  $p(i, j)$  is the pixel value at point  $(i, j)$ ,  $m$  and  $\sigma$  are the mean and standard deviation respectively.

#### Energy

Energy returns the sum of squared elements in the Grey Level Co-Occurrence Matrix (GLCM). The range of energy is  $[0, 1]$ . Energy is 1 for a constant image. The formula for finding energy is given in below equation:

$$E = \sum_{i, j} P(i, j)^2$$

#### Results:

A total of 60 female breast patients were enrolled in this study, in addition to 10 control female (with no symptoms of breast disease). The patients were divided into two main groups; each group included 20 female patients. One group was of benign tumors and the other group of malignant changes. All groups (including the control group) were submitted to mammographic and ultrasound breast examination followed by surgical biopsy, for the breast patients only. Table 1, describes the frequency and age range of each sub-group, and means age  $\pm$  SD, for both (Benign) and (Malignant) groups.

**Table (1): Patients Age Ranges Enrolled in This Work**

Age range	Malignant		Benign	
	Mean	S.D.	Mean	S.D.
(30-45) years	36.40	2.97	36.28	5.18
(46-61) years	35.36	4.45	51.08	5.11
(62-77) years	66.40	3.36	70.00	2,01

**Mammographic Images**

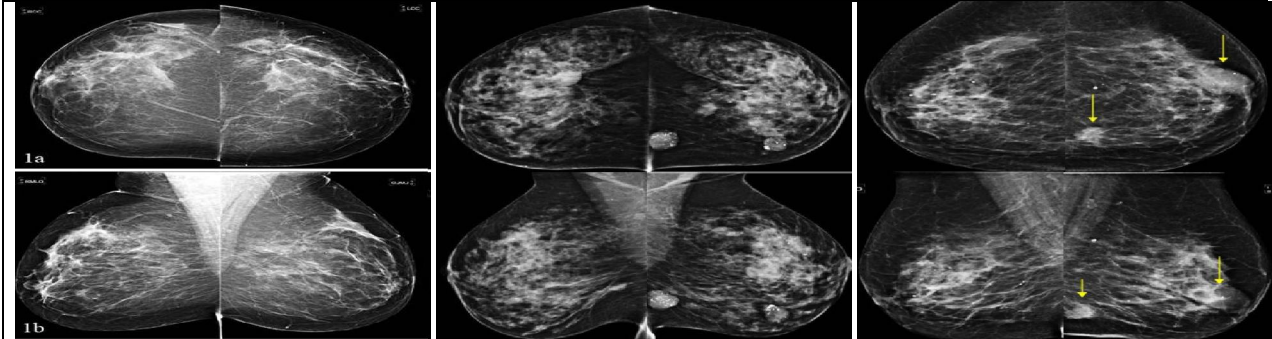


**Figure (1):** Normal mammograms of breast images. (a) Cranio-Caudal (CC) and (b): Mediolateral Oblique (MLO)

**Figure (2):** Benign mammograms of breast images. (a) Cranio-Caudal (CC) and (b): Me diolateral Oblique (MLO) calcified fibroadenoma benign tumors mammography images.

**Figure (3):** Malignant mammograms of breast images. (a) Cranio-Caudal (CC) and (b): Mediolateral Oblique (MLO) Infiltrating ductal carcinoma breast cancer mammography

**Ultrasonography of breast images**

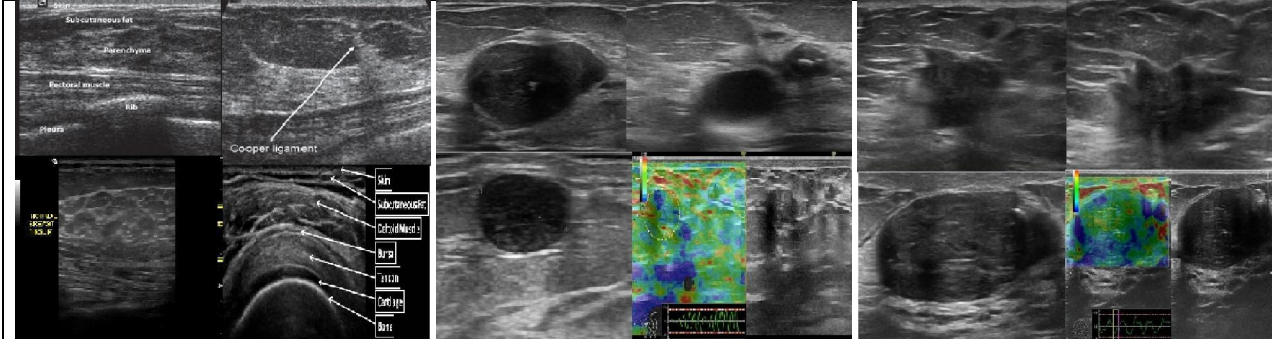
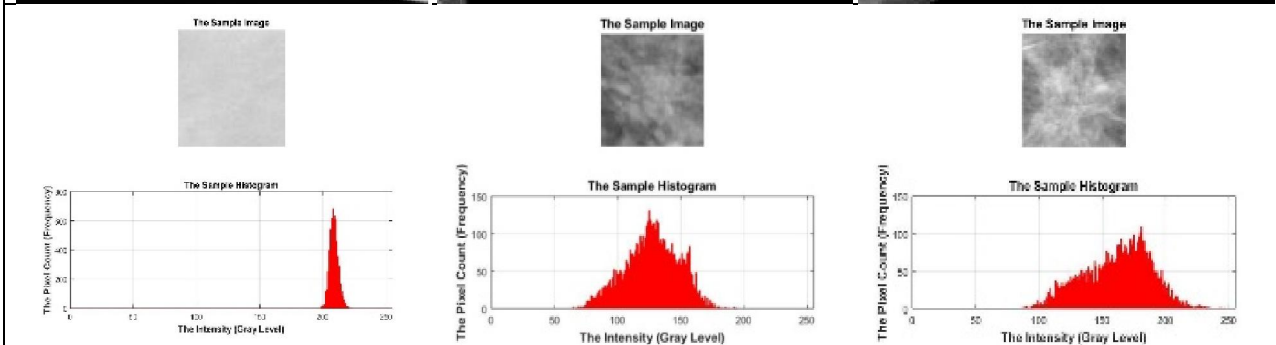
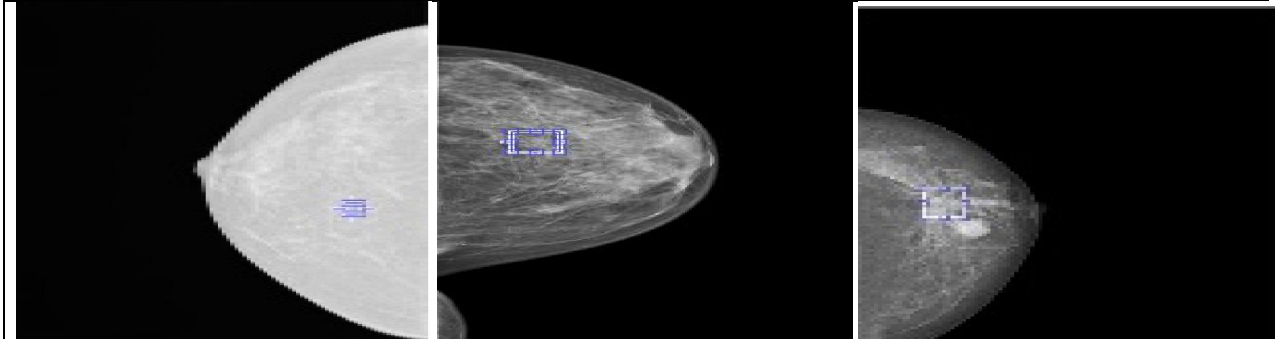


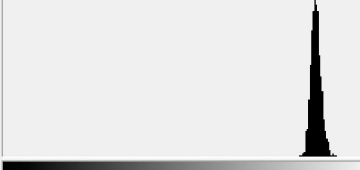
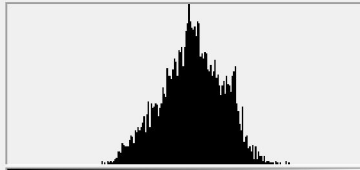
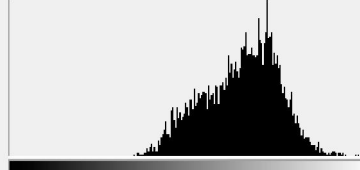
**Figure (4):** Normal breast ultrasound images.

**Figure (5):** Benign breast Ultrasound images calcified fibroadenoma benign tumors ultrasound images.

**Figure (6):** Malignant breast Ultrasound images Infiltrating ductal carcinoma breast cancer.

**Mammographic Images, and the histograms Data (MATLAB and Photoshop 7.0 ME analysis)**



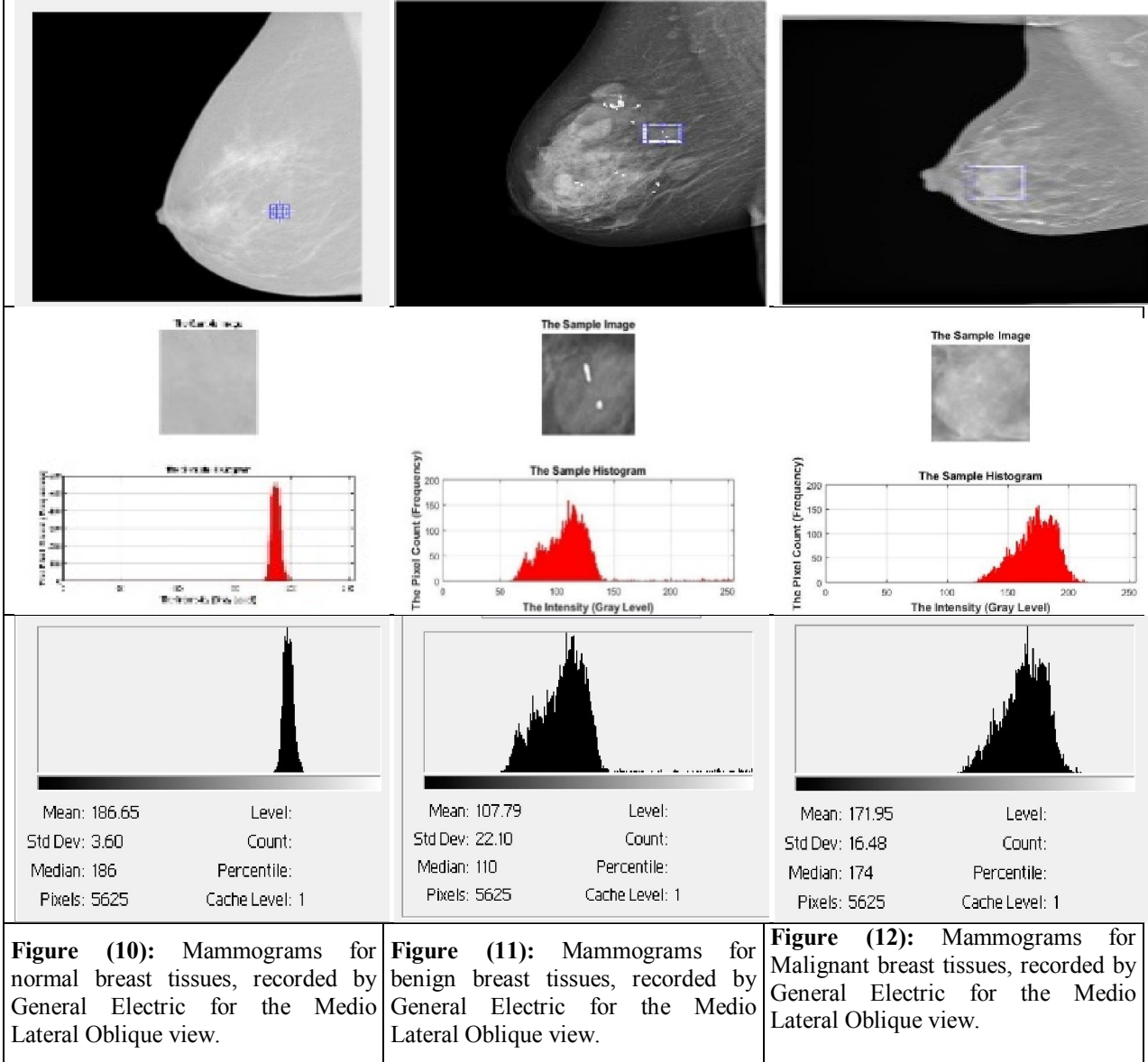
 <p>Mean: 208.71      Level: Std Dev: 3.40      Count: Median: 209      Percentile: Pixels: 5625      Cache Level: 1</p>	 <p>Mean: 127.27      Level: Std Dev: 21.25      Count: Median: 128      Percentile: Pixels: 5625      Cache Level: 1</p>	 <p>Mean: 161.64      Level: Std Dev: 26.49      Count: Median: 165      Percentile: Pixels: 5625      Cache Level: 1</p>
---	--	--

**Figure (7):** Mammograms for normal breast tissues, recorded by General Electric for the cranio-cuadal view. (MATLAB and Photoshop 7.0 ME analysis)

**Figure (8):** Mammograms for benign breast tissues, recorded by General Electric for the cranio-cuadal view. MATLAB and Photoshop 7.0 ME analysis)

**Figure (9):** Mammograms for malignant breast tissues, recorded by General Electric for the cranio-cuadal view. MATLAB and Photoshop 7.0 ME analysis)

**Mammographic Images, and the histograms Data (General Electric)**



Figures (1) to (13), illustrate the collected data from the histograms of each region of interest (ROI) taken from the breast mammograms for the control,

and the breast tumor patients using General Electric mammography system.

**Ultrasonography Images, and the histograms Data**

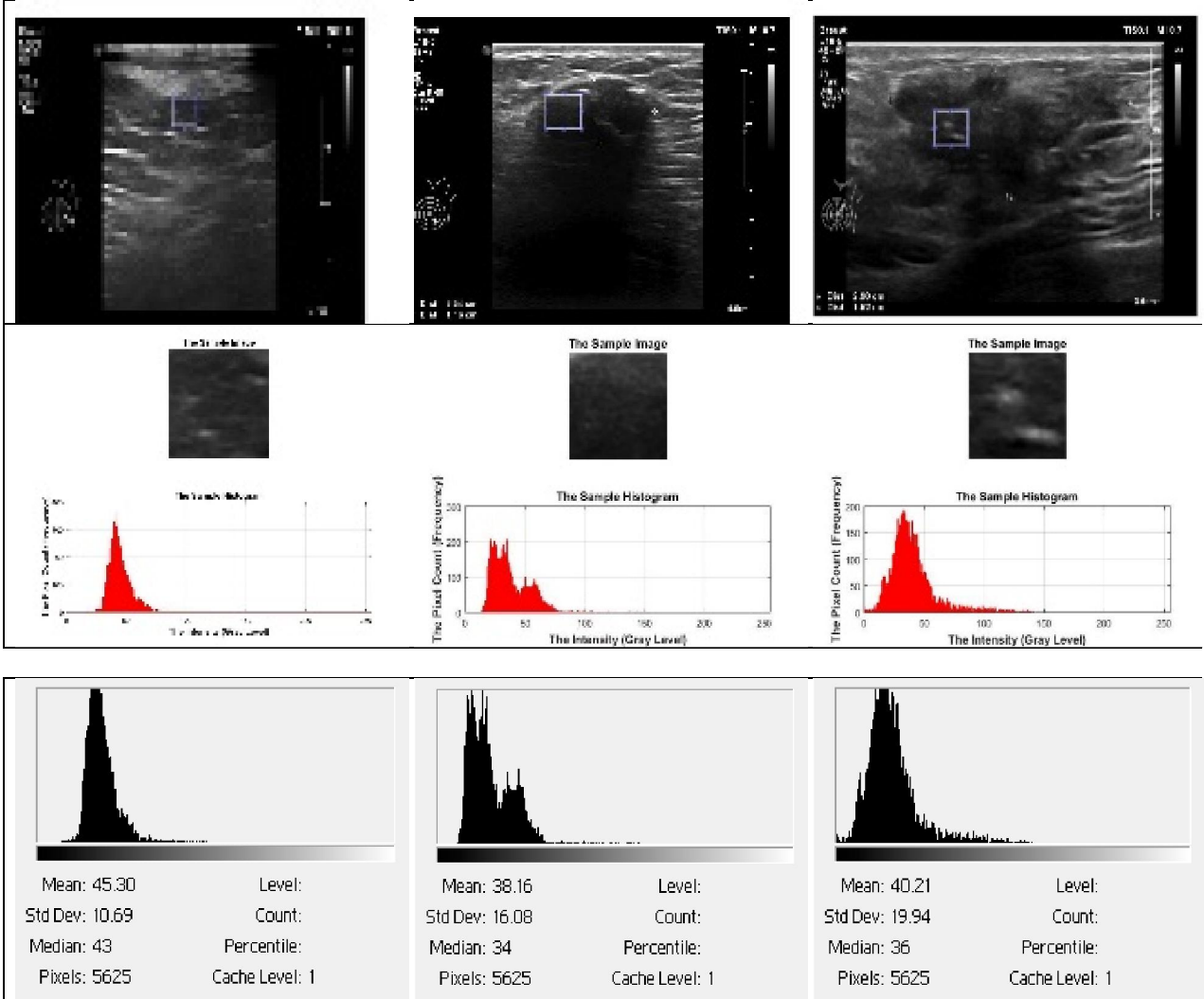


**Figure (13):** Three ultrasounds for Normal breast tissues, recorded by Toshiba for the ultrasounds Image.

**Figure (14):** Three ultrasounds for Benign breast tissues, recorded by Toshiba for the ultrasounds Image

**Figure (15):** Three ultrasounds for Malignant breast tissues, recorded by Toshiba for the ultrasounds Images.

**Table (2): Summary of sensitivities and Specificities (Malignant –Benign) for Mammography, and ultrasound.**

Exam Name	Malignant		Benign	
	The Sensitivity	The specificity	The Sensitivity	The specificity
CC Malignant	98.4286%	87.5%	83.3333%	60%
MLO Malignant	70.3704%	90%	62.5%	90%
US Malignant	84.0769%	69.2308%	73.0769%	69.2308%

**Table (3): Comparison between the three studied groups according to (Mean - standard deviation - median and coefficient of variation) of different parameters using Photoshop program**

Tests	Normal	Benign	Malignant	F	p	Pairwise comparison		
						p <sub>1</sub>	p <sub>2</sub>	p <sub>3</sub>
Ultrasound (Mean)	61.22±15.76	43.54±22.41	54.28±15.53	4.059*	0.022*	0.031	0.608	0.138
CC (Mean)	180.0±22.70	153.4±33.84	154.0±27.87	2.856	0.066	-	-	-
MLO (Mean)	176.9±22.93	158.7±33.68	152.5±27.88	2.134	0.127	-	-	-
Ultrasound (S.D)	13.21 ± 6.69	13.10 ± 6.98	17.62 ± 5.83	3.162	0.060	-	-	-
CC (S.D)	4.79 ± 1.71	19.45±11.11	17.96 ± 6.62	9.648*	<0.001*	<0.001*	0.002*	0.829
MLO (S.D)	5.69 ± 1.60	18.23± 11.10	17.64 ± 9.21	6.855*	0.002*	0.002*	0.007*	0.975
Ultrasound (Median)	60.45±15.85	41.71±21.99	52.40 ± 16.0	4.456*	0.016*	0.020*	0.509	0.138
CC (Median)	176.6±22.13	152.9±35.60	153.2±29.32	2.069	0.136	-	-	-
MLO (Median)	176.8±23.04	158.0±35.09	151.3±29.64	2.126	0.128	-	-	-
Ultrasound (coefficient of variation)	0.21 ± 0.06	0.33 ± 0.17	0.35 ± 0.13	3.720*	0.030*	0.045*	0.034*	0.932
CC (coefficient of variation)	0.03 ± 0.01	0.14 ± 0.11	0.12 ± 0.06	6.515*	0.003*	0.002*	0.019*	0.674
MLO (coefficient of variation)	0.03 ± 0.01	0.13 ± 0.10	0.13 ± 0.08	5.089*	0.009*	0.008*	0.025*	0.965

**Table (4): Comparison between the three studied groups according to (Mean - standard deviation - median and coefficient of variation) of different parameters using MATLAB program**

Mean	Normal	Benign	Malignant	F	p	Pairwise comparison		
						p <sub>1</sub>	p <sub>2</sub>	p <sub>3</sub>
Ultrasound (Mean)	60.56±15.05	39.23±22.07	54.29±15.47	7.536*	0.001*	0.004*	0.653	0.016*
CC (Mean)	175.3±20.84	159.5±33.98	151.4±27.82	2.232	0.115	-	-	-
MLO (Mean)	176.8±22.83	164.3±32.55	151.5±27.45	2.521	0.087	-	-	-
Ultrasound (S.D)	12.81 ± 4.48	13.40 ± 7.31	18.41 ± 4.49	4.964*	0.010*	0.956	0.043*	0.012*
CC (S.D)	4.78±1.52	17.98±10.54	17.65±6.85	10.562*	<0.001*	<0.001*	<0.001*	0.989
MLO (S.D)	5.67 ± 1.65	17.45 ±10.93	17.43 ± 9.03	6.326*	0.003*	0.003*	0.007*	1.000
Ultrasound (Median)	59.83±15.46	37.53±21.83	52.50±15.98	7.925*	0.001*	0.002*	0.559	0.017*
CC (Median)	174.8±20.98	158.9±35.57	150.7±29.38	2.087	0.132	-	-	-
MLO (Median)	176.5±22.93	163.5±34.27	150.5±29.08	2.415	0.096	-	-	-
Ultrasound (coefficient of variation)	0.21 ± 0.04	0.42 ± 0.29	0.36 ± 0.10	4.160*	0.020*	0.015*	0.157	0.596
CC (coefficient of variation)	0.03 ± 0.01	0.13 ± 0.10	0.12 ± 0.06	6.674*	0.002*	0.002*	0.007*	0.969
MLO (coefficient of variation)	0.03 ± 0.01	0.12 ± 0.10	0.12 ± 0.08	4.363*	0.016*	0.015*	0.028*	0.997



**Table (5): Comparison between the three studied groups according to maximum value of different parameters using MATLAB program**

Maximum value	Normal	Benign	Malignant	F	p	Pairwise comparison		
						p <sub>1</sub>	p <sub>2</sub>	p <sub>3</sub>
Ultrasound (Maximum value)	113.0 ± 26.93	105.0 ± 54.91	136.0 ± 47.14	2.728	0.072	-	-	-
CC (Maximum value)	194.2 ± 21.57	223.08 ± 25.67	208.3 ± 30.84	5.663*	0.005*	0.007*	0.333	0.108
MLO (Maximum value)	197.9 ± 24.32	223.2 ± 24.47	202.15 ± 24.26	7.795*	0.001*	0.011*	0.895	0.005*
Ultrasound (Minimum value)	29.92 ± 9.54	29.92 ± 9.54	29.92 ± 9.54	8.605*	<0.001*	0.001*	0.001*	0.989
CC (Minimum value)	11.90 ± 12.22	11.90 ± 12.22	11.90 ± 12.22	7.208*	0.001*	0.005*	0.001*	0.620
MLO (Minimum value)	162.55 ± 21.35	162.55 ± 21.35	162.55 ± 21.35	5.617*	0.005*	0.026*	0.004*	0.356
Ultrasound (Skevnness value)	0.50 ± 0.58	0.50 ± 0.58	0.50 ± 0.58	0.756	0.473	-	-	-
CC (Skevnness value)	0.81 ± 0.88	0.81 ± 0.88	0.81 ± 0.88	1.277	0.285	-	-	-
MLO (Skevnness value)	1.19 ± 0.64	1.19 ± 0.64	1.19 ± 0.64	0.254	0.776	-	-	-
Ultrasound (Energy)	1.0 ± 0.0	0.94 ± 0.141	0.10 ± 0.02	2.746	0.071	-	-	-
CC (Energy)	1.0 ± 0.0	1.0 ± 0.0	1.0 ± 0.0	-	-	-	-	-
MLO (Energy)	1.0 ± 0.0	1.0 ± 0.0	1.0 ± 0.0	-	-	-	-	-

F: F value for ANOVA test, Pairwise comparison bet. each 2 groups was done using Post Hoc Test (Tukey)

p: p value for comparing between three groups. p<sub>1</sub>: p value for comparing between Normal and Benign

p<sub>2</sub>: p value for comparing between Normal and Malignant. p<sub>3</sub>: p value for comparing between Benign and Malignant. \*: Statistically significant at  $p \leq 0.05$

### Discussions:

Due to the high volume of mammograms to be read by physicians, the accuracy rate tends to decrease, and automatic reading of double reading of mammograms, i.e., consecutive reading by two physicians or radiologists, increased the accuracy, but at high costs. That is why the computer aided diagnosis systems are necessary to assist the medical staff to achieve high efficiency and effectiveness. (7-8). In this respect, image analysis techniques played and still played an important role in several medical applications, including enhancing x-ray images, detecting lines in images, transmission and encoding, microscopic imaging, character recognition, and others. (9,10,11). For this purpose, several techniques related to diagnosis and breast tumors differentiation have been developed for detecting abnormalities using image possessing techniques. (12-13)

In the present work, mammography, and ultrasonography image features were used to differentiate between normal, benign and malignant

breast tumors. The comparison and differentiation between normal, benign and malignant breast tumors, in each technique, were followed, based on the gray level histogram, and more precisely, the gray-level co-occurrence histogram (GLCH), using the local binary pattern (LBP), with the region of interest in each technical image was extracted manually.

The images were stored in the digital scan converter of the machines (image memory storage area). A typical digital memory is configured with an image-matrix memory size of 512 x 512 which represents the number of rows and columns of digital picture elements, or pixels. Each pixel in a 512 x 512 matrix represents a specific shade of gray level. The histogram of each image is computed by recording the number of times each pixel's intensity within the valid range appears in the image. For an eight-bit image, the histogram contains 8-bits which gives  $(2^8) = 0-255$  gray-scale levels (256 values,) and that with 12-bit image, the histogram will contain  $2^{12}$  gray-scale levels which gives 4096 values, and so on. The images

obtained from each technique were stored in the digital scan converter as 8-bits which gives  $(2^8) = 0-255$  gray-scale levels. All digitized images were processed off-line by transferring the images to a PC for performing a histogram analysis using two programs software, namely; (Adobe Photoshop 7.0 ME), and MATLAB as image analysis tools. <sup>(142)</sup> MATLAB allows matrix manipulations, plotting of functions and data, implementation of algorithms, creation of user interfaces, and interfacing with programs written in other languages, including C, C++, and FORTRAN. By using both the two programs software (Adobe Photoshop 7.0), and MATLAB Image Processing Toolboxes, differentiation and comparison between the different breast tissues were accomplished. It is of importance to mention that, after selecting the ROIs, histograms were generated and their describing features were calculated at the same time. The histogram parameters were generally used as descriptors of the shape and profile histograms. They were chosen based on the results of similar studies that used histogram parameters for differentiating other tumors types. <sup>(14-15)</sup>

The histogram data of the ROI of each image consists of: i) Number of bands in the histogram, ii) Number of bins for each band of the image, iii) Lowest value checked for each band, and iv) Highest value checked for each band. In Cranio-Caudal or MedioLateral oblique views, benign breast tissue appear as a broad peak of high gray-level at the middle of the histogram, with broad base and sharp top, which clearly differs from the histograms of normal tissue. At the same time, more range, and consequently, more area is occupied by the benign breast tissues due to the wide variations in the benign breast tissues, especially because the types of benign breast tumors are numerous including fibro adenomas, Periductal mastitis, Fat necrosis, Lobular neoplasia, fibrocystic change, areas of thickening, and others. <sup>(16, 17)</sup> The distribution curve is slightly skewed to right which is called (+) skewed. Malignant breast tissue in Cranio-Caudal or MedioLateral oblique views appears as a peak broad of high gray-level at the middle of the histogram, with broad base and broad top, which clearly differs from the histogram of either normal or benign tissue. This characteristic broad peak of malignant breast tissue also occupies more area in the middle of the histogram gray-level especially the broad peak because of the numerous types of breast cancer categories ranging from; Non-Invasive Breast Cancer, Invasive Breast Cancer, Lobular carcinoma in situ (LCIS), Ductal carcinoma in situ (DCIS0), and Infiltrating ductal carcinoma (IDC). <sup>(18)</sup> However, these peaks are characterized by long tail from the lower left level extended to the high right level. The

distribution curve is skewed to left which is called (-) skewed.

Normal breast tissue appears as a sharp peak of high gray-level at the lower end of the histogram, with positive kurtosis <sup>(19,20)</sup>. Accordingly, this is an important difference between the gray-level histograms of normal breast tissues in both US images and breast mammograms. Benign breast tissue appears as a peak with broad base and relatively sharp top with peaks and vales, with the histogram main peak extends from the middle and shifted to the left, i.e. the distribution curve is skewed to left which is called (-) skewed. The histogram of malignant breast tissue appears as a peak with sharp top extends from the middle of the gray-level scale shifted to the left, i.e. the distribution curve is skewed to left which is called (-) skewed.

In the quantitative comparison, the intensity measurements measure the gray-scale statistics in the ROIs. However, in considering the sensitivity and specificity, it is clear that, sensitivity increases on the expense of specificity, and vice versa. The data of this study revealed that, both mammographies has high sensitivity, with ultrasonography is lower. This is because the acoustic characteristics of benign and malignant lesions are overlapping. Ultrasound specificity in breast cancer characterization is low. This is because the acoustic characteristics of benign and malignant lesions are overlapping. Results showed that no imaging method has perfect sensitivity and perfect specificity for the diagnosis of breast cancer.

#### **In conclusion:**

The behavior and the general shape of the gray-level histogram describe specific behavior with each category of tissue, namely; normal, benign and malignant, because each modality gives specific shape for each imaged ROI of each tissue category. As a final conclusion, no single imaging method has perfect sensitivity and perfect specificity for the diagnosis of breast cancer. Accordingly, the choice depends on many factors that take into considerations the limitations, advantages and disadvantages of each modality that is coincide with the patient abilities

#### **References**

1. Tabar L. and Dean P.B. Gynaecol Obstet, 2003; 82, 319-326.
2. Siu AL; U.S. Preventive Services Task Force. Screening for breast cancer: U.S. Preventive Services Task Force recommendation statement. *Annals of Internal Medicine* 2016; 164(4):279–96.
3. Oeffinger KC, Fontham ET, Etzioni R, Herzig A, Michaelson JS, Shih YC, Walter LC, Church

- TR, Flowers CR, LaMonte SJ, Wolf AM, DeSantis C, Lortet-Tieulent J, Andrews K, Manassaram-Baptiste D, Saslow D, Smith RA, Brawley OW, Wender R; American Cancer Society. Breast cancer screening for women at average risk: 2015 guideline update from the American Cancer Society. *JAMA* 2015; 314(15):1599–1614.
4. Kolb TM, Lichy J, Newhouse JH. Comparison of the performance of screening mammography, physical examination, and breast US and evaluation of factors that influence them: an analysis of 27,825 patient evaluations. *Radiology* 2002; 225:165–75.
  5. Moss HA, Britton PD, Flower CD, Freeman AH, Lomas DJ, Warren RM. How reliable is modern breast imaging in differentiating benign from malignant breast lesions in the symptomatic population? *Clin Radiol* 1999; 54:676–82.
  6. Gomez W, Pereira WC, Infantosi AF. Analysis of co-occurrence texture statistics as a function of gray-level quantization for classifying breast ultrasound. *IEEE Trans Med Imaging* 2012;31:1889–99.
  7. Balleyguier C, Kinkel K, Fermanian J, Malan S, Djen G, Taourel P, Helenon O. Computer-aided detection (CAD) in mammography: Does it help the junior or the senior radiologist? *Eur J Rad* 2005;54:90-6.
  8. Brem RF, Hoffmeister JW, Rapelyea JA, Zisman G, Montashemi K, Jindal G, Disimio MP, Rogers SK. Impact of breast density on computer-aided detection for breast cancer. *Am J Roentgenol*. 2005;184:439-44.
  9. Bishop CM: *Pattern Recognition and Machine Learning*. Springer Verlag, Singapore, 2006.
  10. The Objective., Rost, F. and Oldfield, R. in *Photography with a Microscope*, Cambridge University Press, Cambridge, United Kingdom, 2000, PP 70-82.
  11. Azriel Rosenfeld, *Picture Processing by Computer*, New York: Academic Press, 1969.
  12. Shanthy S, Muralibhaskaran V; " Automatic Detection and Classification of Microcalcification, Mass, Architectural Distortion and Bilateral Asymmetry in Digital Mammogram, *International Journal of Medical, Health, Pharmaceutical and Biomedical Engineering* 2014; 8(11):764-69.
  13. Dong M, Zhang J, and Ma Y. "Image denoising via bivariate shrinkage function based on a new structure of dual contourlet transform," *Signal Processing* 2015;109: 25–37.
  14. Just N. Improving tumour heterogeneity MRI assessment with histograms. *Br J Cancer* 2014; 111(12):2205-13.
  15. Chandarana H, Rosenkrantz AB, Mussi TC, Kim S, Ahmad AA, Raj SD, et al. Histogram analysis of whole-lesion enhancement in differentiating clear cell from papillary subtype of renal cell cancer. *Radiology* 2012; 265(3):790-8.
  16. Downey K, Riches SF, Morgan VA, Giles SL, Attygalle AD, Ind TE, et al. Relationship between imaging biomarkers of stage I cervical cancer and poor-prognosis histologic features: quantitative histogram analysis of diffusion-weighted MR images. *AJR Am J Roentgenol* 2013; 200(2):314-20.
  17. Figueroa JD, Pfeiffer RM, Brinton LA, Palakal MM, Degnim AC, Radisky D et al. Standardized measures of lobular involution and subsequent breast cancer risk among women with benign breast disease: a nested case-control study. *Breast Cancer Research & Treatment* 2016; 159(1):163-72.
  18. Nassar A, Visscher DW, Degnim AC, Frank RD, Vierkant RA, Frost M et al. Complex fibroadenoma and breast cancer risk: a Mayo Clinic Benign Breast Disease Cohort Study. *Breast Cancer Research & Treatment* 2015; 153(2):397-405.
  19. National Cancer Institute. *Breast Cancer Treatment During Pregnancy (PDQ)*. 2019. Accessed at [www.cancer.gov/types/breast/hp/pregnancy-breast-treatmentpdq#section/all](http://www.cancer.gov/types/breast/hp/pregnancy-breast-treatmentpdq#section/all) on August 26, 2019.
  20. Venkataraman S, Slanetz PJ. Breast imaging for cancer screening: Mammography and ultrasonography. *UpToDate*. 2019. Accessed at <https://www.uptodate.com/contents/breast-imaging-for-cancer-screeningmammography-and-ultrasonography> on August 26, 2019.

6/16/2020